Aging in the shear-transformation-zone theory of plastic deformation

Jörg Rottler*
Department of Physics and Astronomy, The University of British Columbia, 6224 Agricultural Road, Vancouver, BC, Canada V6T 1Z1

Philipp Maass
Institut für Physik, Technische Universitäty Ilmenau, 98684 Ilmenau, Germany

(Received 24 July 2008; published 24 November 2008)

Aging phenomena in the plastic response of amorphous solids are studied within the theory of shear transformation zones (STZs), which describes the kinetic rearrangement of localized defects in response to external stress. To account for the slow, nonequilibrium dynamics after a quench below the glass transition temperature, two possible models are considered. In the first model, transition rates between the internal states of STZs decrease with time, while in the second model aging occurs due to the relaxation of an effective temperature that determines the number density of STZs and other out-of-equilibium degrees of freedom. It is shown that for reasonable choices of parameters, both models capture qualitatively typical aging features seen in computer simulations and experiments: (i) compliance curves measured for different waiting times t_w after the quench can be superimposed, when the observation times are rescaled with relaxation times $\propto t_w^{\mu}$, $0<\mu \leqslant 1$, and (ii) stress-strain curves show a stationary plateau stress independent of t_w and a peak stress that increases logarithmically with both t_w and the strain rate. Trends of the aging behavior with the quench temperature are also discussed.

DOI: 10.1103/PhysRevE.78.056109 PACS number(s): 81.40.Lm, 83.50.−v, 62.20.F−

I. INTRODUCTION

Whereas in crystalline solids, plastic flow can be ascribed to the motion of dislocations, in amorphous solids, deformation and yield should be related to the dynamics of localized defect structures. Corresponding phenomenological defect-flow theories developed 30–40 years ago [1–3] have been extended recently by Langer and co-workers to the shear-transformation zone (STZ) theory of amorphous plasticity [4–9]. The STZ theory has been very successful in accounting for the mechanical behavior of glassy solids and therefore provides a promising basis for further developments.

STZs are regions containing a few molecules that kinetically rearrange into preferred, locally anisotropic configurations (internal states) with respect to an applied external stress field. Due to the rearrangements, a repopulation of internal states of the STZs occurs, which allows the theory to account for memory effects as seen in numerous experiments and reported already more than 120 years ago in connection with a reduction of the elasticity limit for reversed loading (Bauschinger effect [10]).

STZs have a finite lifetime and can be created and annihilated with rates irrespective of their internal state and proportional to the dissipated energy during loading [11]. This intriguing feature introduces a kind of feedback mechanism and leads to nonlinear rate equations for the population densities of STZ states. The theory predicts a transition from a jammed to a flowing state when the applied stress exceeds a critical value of the order of the yield stress [6]. Below the critical stress, the strain rate never becomes large enough to produce sufficiently strong dissipation for continuous creation of new "unjammed" STZs. As a result, the system reaches a jammed state, where the strain rate becomes zero and the population of the internal STZ states is in kinetic equilibrium with the external loading. Above the critical stress, however, new STZs with internal states independent of the stress field are constantly created by the dissipated plastic energy, and a stationary flow with constant strain rate is reached due to the repopulation of these freshly generated states into internal states with preferred alignment. In addition to fluctuations caused by dissipation, STZs can be created and annihilated by thermal fluctuations [7]. The thermal rate for these spontaneous processes is assumed to be comparable to the rate of the main structural relaxation process of the system.

In recent years, the STZ theory was further developed to account for the behavior seen in systems with slow nonequilibrium dynamics, as, for example, metallic and polymeric glasses [7,9]. To this end, a Boltzmann probability for the occurrence of an STZ was considered with an effective disorder temperature different from the bath temperature. The effective temperature determines the change of configurational entropy with the mean energy of the out-of-equilibrium degrees of freedom. While spontaneous processes with a thermal rate tend to drive the effective temperature to the bath temperature, plastic deformations under loading tend to drive the effective temperature to a different temperature corresponding to a nonequilibrium stationary state of the system.

The concept of an effective temperature involves physics going beyond the very problem of plastic flow in amorphous solids. The effective temperature has been shown to be a fruitful concept in model studies of out-of-equilibrium dynamics [12] and in simulations of glassy materials under steady shear [13–16]. A recent simulation study of shear banding has provided direct numerical evidence for the existence of an effective temperature in amorphous solids [17]. So far, however, the necessary requirements for its validity, its detailed implementation in the evolution equations, and its limitations cannot be derived from general principles.

*jrottler@phas.ubc.ca

Therefore, one is dependent on certain *Ansätze* and their verification in each situation under investigation.

The aim of this work is to study the possibility of describing slow out-of-equilibrium dynamics in the rheology of glassy systems within or by simple extensions of the STZ theory. To this end, we will consider two possible models. In the first one, discussed in Sec. III, no effective temperature is introduced. The slowing down of the dynamics with the system's age is described by an overall increase of the structural relaxation time τ, which, as a primary rate τ^{-1}, enters the transition rates between STZ states. It is assumed that under loading, the energy dissipation due to plastic work drives the relaxation time to a limiting value τ_∞ when reaching a stationary state. In the second model, discussed in Sec. IV, the concept of an effective temperature is followed in the form proposed in the most recent version of the STZ theory [9].

Throughout the paper, we will rely on the simplified two-state version of STZ theory, where in a two-dimensional geometry under pure shear, STZs can be elongated only along two principal axes of the deviatoric stress tensor. As shown in [9], more general situations requiring a tensorial formulation may be essentially reduced to the two-state description, if the distribution of the variables characterizing the STZ states (orientation, size, transition barriers, etc.) is sufficiently narrow to allow for a replacement of disorder averages by representative values.

Our goal is to capture the typical aging behavior found in two standard protocols, which we will call the stress-step protocol and the constant-strain-rate protocol. In the stress-step protocol, the material is quenched to a fixed temperature T below the glass transition temperature T_g at zero time, and exposed to a constant stress σ_{ext} after a waiting time t_w. Thereafter, the shear deformation $\epsilon(t,t_w)$ or compliance $J(t,t_w)=\epsilon(t,t_w)/\sigma_{ext}$ is followed as a function of the observation time t. In the constant-strain-rate protocol, the system is sheared with a fixed rate $\dot{\epsilon}_{ext}$ after t_w and the deviatoric stress $\sigma(\epsilon,t_w)$ is followed as a function of the observation time t or accumulated strain $\epsilon=\dot{\epsilon}_{ext}t$. In the following section, we first describe the typical features seen in such protocols as recently explored in detail by molecular-dynamics simulations [18] of the Kob-Andersen model (80/20 Lennard-Jones mixture) [19] and a bead-spring model of polymers [20] by one of the authors.

II. AGING BEHAVIOR IN THE PLASTIC DEFORMATION OF GLASSY MATERIALS

In the stress-step protocol, for observation times t larger than some microscopic time t_0, the plastic compliance $[J_{pl}(t,t_w)=J(t,t_w)-1/2E$, where $1/2E$ is the elastic part with E the shear modulus] is found to follow a scaling behavior,

$$J_{pl}(t,t_w)=F\left(t_0^{\mu-1}\frac{t_{eff}(t,t_w;\mu)}{t_w^{\mu}}\right), \tag{1}$$

where $F(\cdot)$ is a scaling function with $F(0)=0$, $\mu\leqslant 1$ is the "aging exponent," and $t_{eff}(t,t_w;\mu)$ is Struik's effective time [21],

$$t_{eff}(t,t_w;\mu)=\int_0^t dt'\frac{t_w^{\mu}}{(t'+t_w)^{\mu}} \tag{2a}$$

$$=\frac{t_w}{1-\mu}\left[\left(1+\frac{t}{t_w}\right)^{1-\mu}-1\right] \tag{2b}$$

$$\sim\begin{cases} t, & t/t_w\ll 1,\\ \dfrac{t^{1-\mu}t_w^{\mu}}{(1-\mu)}, & t/t_w\gg 1. \end{cases} \tag{2c}$$

According to this expression, aging effects in the response (1) disappear for $t/t_w\gg 1$. The exponent μ usually depends on the applied stress and the temperature, $\mu=\mu(\sigma_{ext},T)$. It typically decreases with increasing σ_{ext}, $\partial\mu(\sigma_{ext},T)/\partial\sigma_{ext}<0$, a behavior sometimes termed "rejuvenation," since in this case larger stresses will lead to a decrease of the characteristic response time $\propto t_w^{\mu}$ of the compliance in the aging regime $t_0\ll t\leqslant t_w$ [22]. Additionally, the aging exponent typically decreases with decreasing $T<T_g$, $\partial\mu(\sigma_{ext},T)/\partial T>0$.

In Refs. [20,23], a reasonable fit to the scaling function was achieved by using a Kohlrausch type law,

$$F(u)=\exp(cu^{\beta})-1, \tag{3}$$

with an exponent $\beta\simeq 0.5$. However, the form of the scaling function and the dependence of μ on σ_{ext} and T usually depend on details of the system. A primary focus in this work will be to see if the generic scaling feature with $t_{eff}(t,t_w;\mu)$ can be recovered by variants of the STZ theory.

Let us finally note that Eq. (1) can be a valid description only for observation times smaller than a crossover time $t_\times$, while beyond $t_\times$ the compliance is expected either to saturate for loads σ_{ext} smaller than the yield stress σ_y, or to increase linearly with t for $\sigma_{ext}>\sigma_y$. However, even for large stresses, the regime $t>t_\times$ usually cannot be reached so that the behavior as described by Eq. (1) gives the accessible information obtained from a stress-step protocol.

In the constant-strain-rate protocol, for sufficiently large shear rates, the deviatoric stress $\sigma(\epsilon,t_w)$ first increases with ϵ up to a peak stress σ_{max} at a shear deformation $\epsilon_{max}=\dot{\epsilon}_{ext}t_{max}$. In monomeric glass formers such as colloidal or metallic glasses, the stress thereafter relaxes toward a plateau stress σ_{ss} when the system reaches a stationary state. In polymer glasses, however, a similar regime of strain softening is followed by strain hardening due to chain entanglements and a true steady state cannot be achieved.

Both the plateau and the peak stress increase monotonously with $\dot{\epsilon}_{ext}$. For short waiting times $t_w<1/\dot{\epsilon}_{ext}$, a logarithmic increase $\propto\ln(\dot{\epsilon}_{ext}t_0)$ is typically found, while for long waiting times $t_w>1/\dot{\epsilon}_{ext}$, σ_{max} and σ_{ss} become almost independent of $\dot{\epsilon}_{ext}$. In the short waiting time regime $t_w<1/\dot{\epsilon}_{ext}$, the overshoot stress $(\sigma_{max}-\sigma_{ss})$ increases as well with $\dot{\epsilon}_{ext}$, meaning that in this regime σ_{max} grows faster with the strain rate than σ_{ss}. At fixed strain rate, the plateau stress is independent of the waiting time. By contrast, the peak stress σ_{max} increases logarithmically with t_w.

The combined dependence of σ_{max} on $\dot{\epsilon}_{ext}$ and t_w was studied in detail in Ref. [18] for the Kob-Andersen model. It was found that for small $t_w\ll\epsilon_{eff}/\dot{\epsilon}_{ext}$, σ_{max} is dominated by

the time $t_{max}=\epsilon_{max}/\dot{\epsilon}_{ext}$ to reach the peak stress, while for $t_w \gg \epsilon_{eff}/\dot{\epsilon}_{ext}$, σ_{max} grows logarithmically with t_w, with an offset increasing with $\ln(\dot{\epsilon}_{ext}t_0)$. The effective shear deformation ϵ_{eff} is of order ϵ_{max} and accounts for the load influence on the aging. In the case of rejuvenation, $\epsilon_{eff}<\epsilon_{max}$, while for overaging, $\epsilon_{eff}>\epsilon_{max}$. The overall behavior can be summarized as

$$\sigma_{max}=\sigma_{max}^{(0)}+\sigma_{max}^{(1)}\ln\left(\frac{t_w}{t_0}+\frac{\epsilon_{eff}}{\dot{\epsilon}_{ext}t_0}\right)+\sigma_{max}^{(2)}\ln(\dot{\epsilon}_{ext}t_0), \quad (4)$$

where $\sigma_{max}^{(i)}$, $i=0,1,2$, are constants independent of t_w and $\dot{\epsilon}_{ext}$, and $\sigma_{max}^{(2)}>\sigma_{max}^{(1)}$. Equation (4) implies that $\sigma_{max}+(\sigma_{max}^{(2)}-\sigma_{max}^{(1)})\ln(t_w/t_0)$ is a function of $\dot{\epsilon}_{ext}t_w$ only.

III. AGING DUE TO SLOWING DOWN OF STZ TRANSITION RATES

Our first approach is motivated by the idea that aging slows down all relevant transitions in the glassy solid. There is clear experimental [21], theoretical [24], and computational [25] evidence that the main structural α-relaxation time τ increases as a power law with wait time t_w in a strongly temperature-dependent manner. Although the molecules find themselves in highly constrained, caged configurations, they are not completely jammed and, at finite temperature, can perform small thermally activated excursions that improve the local packing. It therefore seems natural to assume that the STZ transition rates are proportional to the inverse of τ, and to supplement the (scalar) STZ equations of motion as formulated in Ref. [6] with an evolution equation for τ. The possibility of time-dependent STZ transition rates has already been suggested by Lemaître in the context of free-volume relaxations [26], but not systematically applied to the aging phenomenology described in Sec. II.

In the scalar STZ theory, the total shear deformation $\epsilon_{tot}=\epsilon_{el}+\epsilon_{pl}$ is the sum of the elastic part $\epsilon_{el}=\sigma/2E$ and the plastic part ϵ_{pl}, which follows the rate equation

$$\dot{\epsilon}_{pl}=\lambda[R_-(\sigma)n_- - R_+(\sigma)n_+], \quad (5)$$

where $n_\pm$ are the number densities of STZ states in the two principal directions, σ is the deviatoric stress, and $R_\pm(\sigma)$ are the transition rates; λ is an elementary volume of order the size of an STZ. The number densities of the STZ states obey the rate equations

$$\dot{n}_\pm = R_\mp(\sigma)n_\mp - R_\pm(\sigma)n_\pm - \Gamma(n_\pm,\sigma)\left(n_\pm-\frac{n_\infty}{2}\right), \quad (6)$$

where Γ is the annihilation rate per STZ and $n_\infty\Gamma/2$ the production rate of STZs per volume in either state due to fluctuations caused by the loading. In Ref. [6], it is suggested that n_∞ is a constant and that Γ is proportional to the dissipated energy density per STZ, i.e., $\Gamma=-\dot{Q}/[\sigma_Q\lambda n_{tot}]$ with $(-\dot{Q})$ the dissipated heat per unit time and volume, $n_{tot}=n_++n_-$ the total STZ density, and σ_Q a characteristic scale of energy density or stress. An explicit expression for $\Gamma=\Gamma(n_\pm,\sigma)$ can be derived by using (i) the first law of thermodynamics, $\dot{U}=\dot{Q}+\dot{W}$, with $\dot{W}=2\sigma\dot{\epsilon}_{pl}$ the plastic work density per unit time and $U=U(n_-,n_+)$ the STZ contribution to the internal energy density; (ii) a scaling *Ansatz* $U(n_-,n_+)=\sigma_Q\lambda n_{tot}\psi(\Delta/n_{tot})$ with $\Delta=n_+-n_-$; and (iii) the requirement that the dissipation rate must be positive according to the second law of thermodynamics [for further details, see Ref. [6] and Eq. (17) below].

In this work, we shall use a semilinearized form [27] of the transition rates,

$$R_\pm(\sigma)=\frac{1}{\tau}\exp\left(\mp\frac{\sigma}{\sigma_0}\right), \quad (7)$$

where σ_0 is a characteristic stress of the order of the yield stress. Our proposed modification consists of an evolution equation for the relaxation time τ,

$$\dot{\tau}=\mu\frac{\tau}{t+t_0}-\nu\frac{n_{tot}}{n_\infty}\Gamma(\tau-\tau_\infty), \quad (8)$$

where ν is a constant. The first term on the right-hand side describes the slowing down of the structural relaxation in the absence of plastic deformation, $\tau=\tau_0(t_w/t_0+1)^\mu\sim\tau_0(t_w/t_0)^\mu$ for $t_w\gg t_0$, where τ_0 is the initial structural relaxation time after the quench. The unlimited increase of τ with t_w in the absence of dissipation refers to the nonequilibrium aging regime, which is of interest in this work. In systems in which the experimental time window covers waiting times t_w exceeding an equilibration time t_{eq}, a modification of Eq. (8) is necessary so that τ approaches a constant value for $t_w\gg t_{eq}$. Such a modification can be done similarly to the incorporation of the thermal relaxation process in the effective temperature formulation of the STZ theory [see Eq. (20) below].

The second term on the right-hand side of Eq. (8) implies that in the presence of dissipation during plastic deformation, the aging process will eventually stop, so that τ attains a steady-state value τ_∞. The rate for approaching this steady-state value is assumed to be proportional to the dissipation rate per volume $-\dot{Q}\propto n_{tot}\Gamma$. By construction, the scalar variable τ acts as a memory carrier of the system. We note that a similar approach to capturing the effects of aging and rejuvenation was proposed in Ref. [28] in the context of an evolution equation for the inverse relaxation time or fluidity in a rheological model for soft glasses.

Since the strain rate dependence of the plateau stress σ_{ss} may in general be different from the rate dependence of the peak stress σ_{max} [i.e., the overshoot $(\sigma_{max}-\sigma_{ss})$ often increases with rate, see Sec. III B below], we further assume that τ_∞ is a function of the total strain rate,

$$\tau_\infty=\tau_0^\infty f(\dot{\epsilon}_{tot}t_0). \quad (9)$$

Specifically, we choose $f(u)=u^{1/2}$ in the following analysis. A simple motivation for this *Ansatz* is the idea that in steady state where the system is constantly stirred, the structural relaxation time will be coupled to the strain rate. The choice of the exponent $1/2$ is arbitrary and could be adjusted to a specific rate dependence of the steady-state flow stress.

We follow the authors of the STZ theory and rewrite Eqs. (5)–(8) in terms of the normalized total STZ density Λ and STZ imbalance m, $0\leq m<1$,

$$\Lambda = \frac{n_{\text{tot}}}{n_\infty} = \frac{n_+ + n_-}{n_\infty}, \quad m = \frac{\Delta}{n_{\text{tot}}} = \frac{n_+ - n_-}{n_+ + n_-}. \tag{10}$$

With $\epsilon_0 = \lambda n_\infty$, these equations then read

$$\dot{\epsilon}_{\text{pl}} = \epsilon_0 \mathcal{C}(\sigma)\Lambda[\mathcal{T}(\sigma) - m], \tag{11}$$

$$\dot{\Lambda} = -\Gamma(\Lambda - 1), \tag{12}$$

$$\dot{m} = 2\mathcal{C}(\sigma)[\mathcal{T}(\sigma) - m] - \Gamma\frac{m}{\Lambda}, \tag{13}$$

$$\dot{\tau} = \mu\frac{\tau}{t + t_0} - \nu\Lambda\Gamma(\tau - \tau_\infty), \tag{14}$$

where we introduced the rate factors

$$\mathcal{C}(\sigma) = \frac{1}{2}[R_-(\sigma) - R_+(\sigma)] = \frac{1}{\tau}\cosh\left(\frac{\sigma}{\sigma_0}\right), \tag{15}$$

$$\mathcal{T}(\sigma) = \frac{R_-(\sigma) - R_+(\sigma)}{R_-(\sigma) + R_+(\sigma)} = \tanh\left(\frac{\sigma}{\sigma_0}\right). \tag{16}$$

The annihilation rate following from the procedure described above is

$$\Gamma(\sigma, \Lambda, m) = \frac{2\mathcal{C}(\sigma)[\mathcal{T}(\sigma) - m][\sigma_Q^{-1}\sigma - \psi'(m)]}{1 - \Lambda^{-1}m\psi'(m) + (\Lambda^{-1} - 1)\psi(m)}. \tag{17}$$

As discussed in [7], this rate remains positive if the numerator of the fraction remains positive, meaning that $[\mathcal{T}(\sigma) - m]$ and $[\sigma_Q^{-1}\sigma - \psi'(m)]$ should change sign at the same pair of values (σ, m). This implies that the inverse function $\mathcal{T}^{-1}(m) = \sigma_0 \text{atanh}(m)$ determines $\psi'(m) = \sigma_Q^{-1}\mathcal{T}^{-1}(m)$ and

$$\psi(m) = \psi_0 + \frac{1}{\sigma_Q}\int_0^m \mathcal{T}^{-1}(m')dm' \tag{18a}$$

$$= \psi_0 + \frac{\sigma_0}{2\sigma_Q}[(1 - m)\ln(1 - m) + (1 + m)\ln(1 + m)], \tag{18b}$$

where ψ_0 is a constant.

Experiments and simulations show that aging is a strongly temperature-dependent phenomenon. As discussed in Sec. II, the aging exponent μ is found to decrease when the temperature is lowered: μ decreases from close to 1 for temperatures just below the glass transition temperature to zero in the limit of $T \to 0$. Furthermore, the initial relaxation time τ_0 will depend on the quench depth and quench rate, typically leading to a strong increase of τ_0 with decreasing T (the temperature after the quench). Also the steady-state relaxation time τ_∞ [or τ_0^∞ in the *Ansatz* (9)] can be expected to increase with decreasing temperature. At this point in the development, we do not wish to make specific assumptions about the functional forms of these temperature dependences. We aim to illustrate below that the correct trends with temperature can emerge from such a theory if one allows the described quantities to vary with T. Specific assumptions can be made when one attempts to fit the theory to specific materials. This might in fact require additional modifications such as thermally activated transition rates (see also Sec. V).

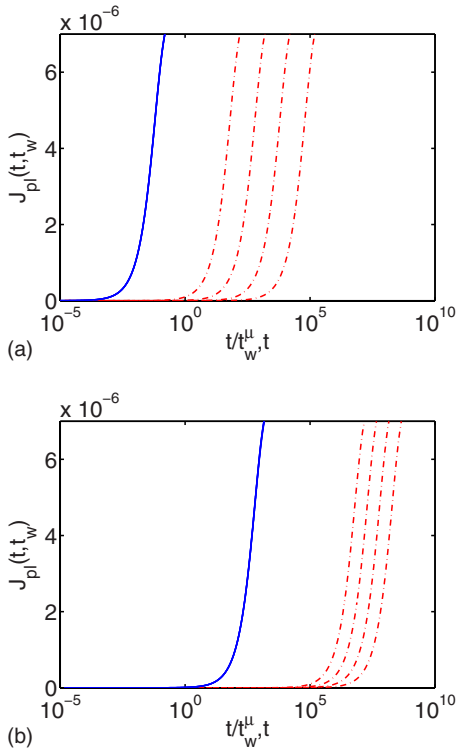

FIG. 1. (Color online) Compliance curves (red, dot dashed) for $\sigma_{\text{ext}} = 0.1$ and two different "temperatures": (a) $t_w = 10^3 - 10^6$, $\mu = 1$, $\tau_0 = 0.1$, and $\tau_0^\infty = 10$; (b) $t_w = 10^8 - 10^{11}$, $\mu = 0.5$, $\tau_0 = 1000$, and $\tau_0^\infty = 100$. The compliance curves collapse onto a common curve (blue, solid) when time is rescaled with t_w^μ.

We now demonstrate that our modified STZ theory is capable of describing all trends of aging effects on the mechanical properties as described in Sec. II. To this end, we take t_0, ϵ_0, and σ_0 as units for the time, strain, and stress, respectively, and solve Eqs. (11)–(14) numerically during the observation time t, starting with the initial conditions $\epsilon_{\text{pl}}(0, t_w) = 0$, $m(0, t_w) = 0$, $\Lambda(0, t_w) = \Lambda_0$, and $\tau(0, t_w) = \tau_0(t_w + 1)^\mu$. In the constant-strain-rate protocol with $\dot{\epsilon}_{\text{tot}} = \dot{\epsilon}_{\text{ext}}$, the set of evolution equations (11)–(14) is supplemented by

$$\dot{\sigma} = 2E(\dot{\epsilon}_{\text{ext}} - \dot{\epsilon}_{\text{pl}}) \tag{19}$$

with the initial condition $\sigma(0, t_w) = 0$. To get an impression of the influence of the temperature, the parameters μ, τ_0, and τ_0^∞ are varied in accordance with the expected trend. For the remaining parameters, a fixed representative set is used in all calculations: $\nu = 1$, $\psi_0 = \Lambda_0$, $\Lambda_0 = 0.01$, and $\sigma_Q = 2E = 1$.

A. Creep compliance

Figure 1 shows several creep compliance curves with shapes typically seen in experiments and simulations. In panel (a) we have chosen $\mu = 1$ and relatively small values of τ_0 and τ_∞. This combination of parameters might represent a temperature just below the glass transition temperature

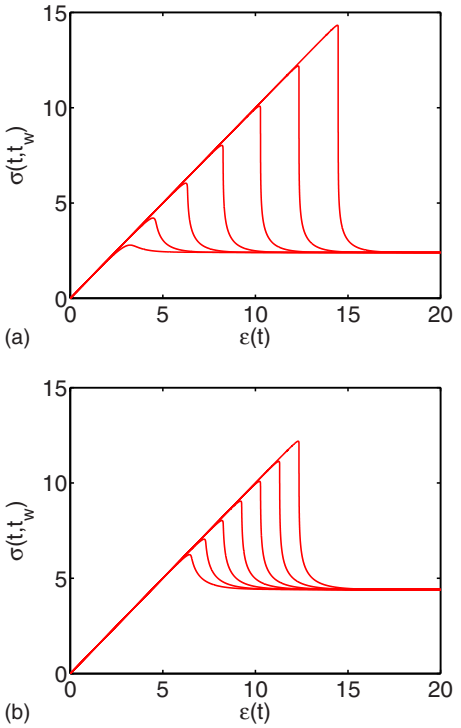

FIG. 2. (Color online) Stress-strain curves for several waiting times $t_w=10^4-10^{10}$ (bottom to top), fixed strain rate $\dot{\epsilon}_{ext}=0.01$ and otherwise the same parameters as in Figs. 1(a) and 1(b), respectively.

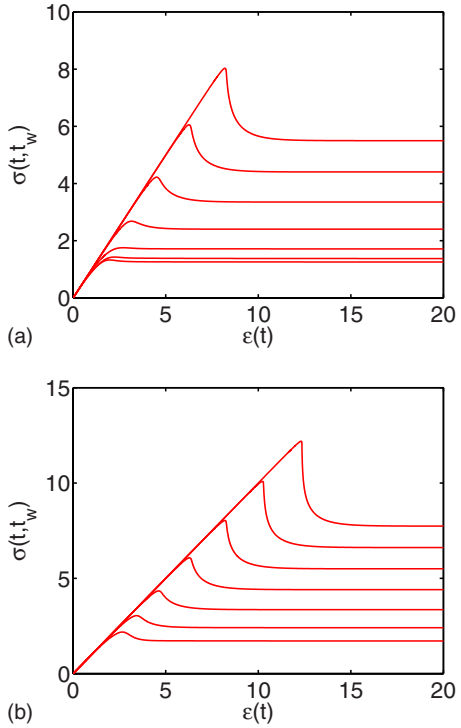

FIG. 3. (Color online) Stress-strain curves for varying strain rates $\dot{\epsilon}_{ext}=10^{-5}-10^{1}$ (bottom to top), fixed $t_w=10^4$ and otherwise the same parameters as is Fig. 1(a) and 1(b), respectively.

where "full" (or "normal") aging is observed. To demonstrate that the theory can also capture trends consistently at lower temperatures, we consider lower values of $\mu=0.5$ in panel (b) and choose a complementary set of relaxation times. For increasing wait times t_w, curves shift to the right on the time axis in both cases, indicating that aging delays the onset of creep. After rescaling time with t_w^{μ}, all curves collapse onto a single curve, which shows that the compliance obeys time-waiting time superposition, a key feature of aging phenomenology. An inspection of the STZ equations of motion shows that this is not surprising since the rate factor $\mathcal{C}(\sigma)$ is the only age-dependent quantity on the right-hand side (rhs) of all equations, including the equation for Γ. All times are therefore rescaled as desired. However, we note that the scaling function does not agree well with the Kohlrausch form Eq. (3).

B. Peak stress

Having established the presence of aging effects in the compliance, we proceed by studying deformation in the constant-strain-rate protocol. Figure 2 shows representative stress-strain curves for the same parameters as in Fig. 1. We observe that the initial elastic response, $\sigma=\epsilon$, is followed by a stress overshoot that increases with increasing t_w. Sustained plastic deformation then reduces the stress from a peak value σ_{max} to a steady-state, history-independent plateau stress σ_{ss}. Our model already captures two major features of aging: an increase of the peak (yield) stress σ_{max} with age and a fully "rejuvenated," age-independent flow stress σ_{ss}.

We now turn to the effect of strain rate at fixed waiting time t_w in Fig. 3. Both σ_{max} and σ_{ss} increase with increasing strain rate, but they differ in rate sensitivity. For $\dot{\epsilon}_{ext}<1/t_w$, both stresses vary weakly with rate and approach limiting values for $\dot{\epsilon}_{ext}\to 0$. For $\dot{\epsilon}>1/t_w$, the rate dependence becomes stronger. At the same time, the overshoot $(\sigma_{max}-\sigma_{ss})$ increases with $\dot{\epsilon}_{ext}$. These trends are again in agreement with the molecular-dynamics simulations in Refs. [18,20,29] and also with experiments; see, e.g., the behavior found for metallic glasses in Ref. [30].

Figure 4(a) shows the peak stress σ_{max} obtained from the stress-strain curves in Fig. 2 as well as two additional values of $\mu=0.75, 0.25$ or "temperatures" as a function of waiting time t_w at fixed $\dot{\epsilon}_{ext}=0.1$ in the regime $t_w>1/\dot{\epsilon}_{ext}=10$. For each temperature, the curves become linear in the semilogarithmic representation for large t_w, meaning that $\sigma_{max}\sim\sigma_{max}^{(1)}\ln(t_w)$ for $t_w\to\infty$ in agreement with Eq. (4). As shown in the inset of Fig. 4(a), the slope $\sigma_{max}^{(1)}$ is proportional to μ. Moreover, when extrapolating the asymptotic lines to $t_w=1$, we can determine their "offset," which, according to Eq. (4), should increase with $\dot{\epsilon}_{ext}$ as $\sigma_{max}^{(0)}+\sigma_{max}^{(2)}\ln(\dot{\epsilon}_{ext})$.

Note that for fixed t_w, the dependence of σ_{max} in Fig. 4(a) is qualitatively different. For small t_w, σ_{max} increases with decreasing "temperature." This is the expected behavior, if aging effects are not present or can be neglected. For large t_w by contrast, which corresponds to a strongly aged system, σ_{max} decreases with decreasing "temperature." In our model, the appearance of this behavior is a consequence of our choice of the relaxation times τ_0. The crossover into this

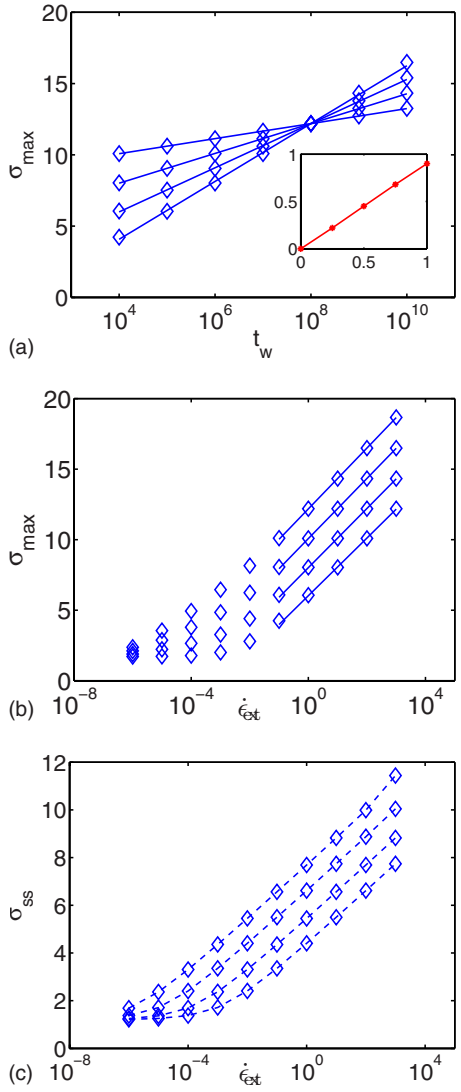

FIG. 4. (Color online) Peak stress σ_{max} (a) as a function of waiting time at fixed $\dot{\epsilon}_{ext}=0.1$, and (b) as a function of strain rate at fixed $t_w=10^4$, for four different "temperatures" represented by ($\mu=1$, $\tau_0=0.1$, $\tau_0^\infty=10$), ($\mu=0.75$, $\tau_0=10$, $\tau_0^\infty=30$), ($\mu=0.5$, $\tau_0=1000$, $\tau_0^\infty=100$), ($\mu=0.25$, $\tau_0=100\,000$, $\tau_0^\infty=300$) (from bottom to top). Solid lines in panel (a) are logarithmic fits with slope $\sigma_{max}^{(1)}$, and $\sigma_{max}^{(1)}$ is plotted against μ in the inset. Solid lines in panel (b) have slope $\sigma_{max}^{(2)}=0.9$ independent of μ. (c) Steady-state plateau stress σ_{ss} as a function of strain rate for the same four temperatures.

regime can easily be controlled by adjusting τ_0, and hence the offset $\sigma_{max}^{(0)}$ of the curves. It would be interesting to see if the existence of this regime can be confirmed in experiments and simulations.

In panel (b) of Fig. 4, the peak stress σ_{max} is analyzed as a function of strain rate $\dot{\epsilon}_{ext}$ at fixed $t_w=10^4$ for the same four different "temperatures" as in panel (a). The data for two "temperatures" $\mu=1$ and 0.5 correspond to the curves shown in Fig. 3. Two regimes of rate dependence emerge: a logarithmic rate dependence at large rates crosses over into vanishing rate sensitivity at lower rates. As the temperature is lowered, the crossover between the two regimes moves to smaller $\dot{\epsilon}_{ext}$. From the slope of the asymptotic lines for large $\dot{\epsilon}_{ext}$, we can determine the constant $\sigma_{max}^{(2)}$ according to Eq. (4).

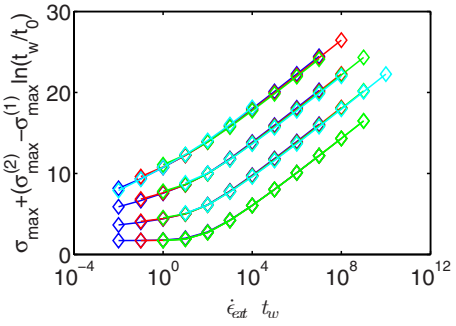

FIG. 5. (Color online) Scaling plot of the peak stress as predicted by Eq. (4) for the four different "temperatures" analyzed in Figs. 4(a) and 4(b).

Another important rheological quantity that one would like to predict with STZ theory is the steady-state plateau stress σ_{ss}. This stress is independent of t_w. Its dependence on $\dot{\epsilon}_{ext}$ is shown in Fig. 4(c). Again, we see two regimes of rate sensitivity, with the crossover moving toward smaller $\dot{\epsilon}_{ext}$ at lower temperatures.

One of the central findings of Ref. [18] was that the peak stress for different rates and waiting times could be superimposed onto a master curve when plotted against the dimensionless quantity $\dot{\epsilon}t_w$ and shifting the peak stress by a waiting time-dependent factor. Using the values $\sigma_{max}^{(1)}$ and $\sigma_{max}^{(2)}$ for each temperature, we can test if $\sigma_{max}+(\sigma_{max}^{(2)}-\sigma_{max}^{(1)})\ln(t_w)$ is a function of $\dot{\epsilon}_{ext}t_w$ only, as predicted by Eq. (4). Corresponding scaling plots are shown in Fig. 5 and compare well with the behavior found in Fig. 3 of Ref. [18].

IV. AGING DUE TO EFFECTIVE TEMPERATURE-CONTROLLED STZ DENSITY

Since its formulation in Ref. [6], STZ theory has undergone a series of developments that have included thermal effects as well as the notion of an effective temperature T_{eff} [7], which controls the limiting value n_∞ of the STZ density. Similar to the relaxation time τ, T_{eff} can be regarded as an additional state variable that encodes the history of the nonequilibrium dynamics of the system. As an alternative approach for describing the aging effects discussed in Sec. II, we consider here the primary rate τ^{-1} in Eq. (7) to be independent of t_w, but n_∞ to be age-dependent according to the most recent version of STZ theory [9] (in scalar formulation). Hence Eq. (8) is irrelevant now and we instead set $\tau \equiv a(T)t_0$, where $a(T)$ is a temperature-dependent prefactor and t_0 a (T-independent) microscopic time, which we continue to use as a time unit.

Compared to the formulation of Ref. [6] used in Sec. III, two extensions have to be considered. The first is the effective temperature concept, which means that the limiting value n_∞ is replaced by $n_\infty \exp(-1/\chi)$, where $\chi=T_{eff}/T_Z$, and $k_B T_Z$ is a typical STZ formation energy. The second extension is that in addition to the fluctuations due to dissipation of mechanical energy, thermal fluctuations give rise to the creation and annihilation of STZs. Denoting the corresponding thermal relaxation rate per STZ by ρ, Eq. (6) becomes

$$\dot{n}_{\pm} = R_{\mp} n_{\mp} - R_{\pm} n_{\pm} - (\Gamma + \rho)\left(n_{\pm} - \frac{n_{\infty}}{2} e^{-1/\chi}\right). \quad (20)$$

With these modifications, one has to replace Γ by $\Gamma_{\mathrm{tot}} = \Gamma + \rho$, $\epsilon_0 = \lambda n_{\infty}$ by $\tilde{\epsilon}_0 = \epsilon_0 \exp(-1/\chi)$, and $\Lambda = n_{\mathrm{tot}}/n_{\infty}$ by $\tilde{\Lambda} = \Lambda \exp(1/\chi)$ in Eqs. (11), (13), and (12). The total annihilation rate becomes

$$\Gamma_{\mathrm{tot}} = \frac{2\mathcal{C}(\mathcal{T} - m)[\sigma_Q^{-1}\sigma - \psi'(m)] + \rho}{1 - \tilde{\Lambda}^{-1} m \psi'(m) + (\tilde{\Lambda}^{-1} - 1)\psi(m)}. \quad (21)$$

To ensure that Γ is positive for $\rho \geqslant 0$, the same $\psi(m)$ from Eq. (18) can be used.

Moreover, as discussed in Ref. [9], the introduction of the effective temperature leads to a separation of time scales: While $\tilde{\Lambda}$ is of order unity according to Eq. (12), $\tilde{\epsilon}$ on the right-hand side of Eq. (11) leads to an additional factor $\propto \exp(-1/\chi) \ll 1$, so that ϵ_{pl} relaxes much slower than Λ and m in Eqs. (12) and (13), respectively. For the time evolution of ϵ_{pl} or σ in Eq. (19), we therefore can use a quasistationary approximation, where $\tilde{\Lambda}$ and m attain their steady-state values $\tilde{\Lambda}_{\infty} = 1$ $[\Lambda_{\infty} = \exp(-1/\chi)]$ and

$$M(\sigma) = \frac{\sigma_Q}{2\sigma}\left\{\left[1 + \frac{\mathcal{T}(\sigma)\sigma}{\sigma_Q} + \frac{\rho}{2\mathcal{C}(\sigma)}\right] - \sqrt{\left[1 + \frac{\mathcal{T}(\sigma)\sigma}{\sigma_Q} + \frac{\rho}{2\mathcal{C}(\sigma)}\right]^2 - 4\frac{\mathcal{T}(\sigma)\sigma}{\sigma_Q}}\right\}. \quad (22)$$

The only remaining dynamical equation is the equation for ϵ_{pl} [and Eq. (19)],

$$\dot{\epsilon}_{\mathrm{pl}} = \epsilon_0 \exp(-1/\chi)\mathcal{C}(\sigma)[\mathcal{T}(\sigma) - M(\sigma)], \quad (23)$$

with

$$\Gamma = \frac{2\mathcal{C}(\mathcal{T} - M)[\sigma_Q^{-1}\sigma - \psi'(M)] + M\psi'(M)\rho}{1 - M\psi'(M)}. \quad (24)$$

A difficult problem is the prediction of the time evolution of T_{eff}, which involves other degrees of freedom than belonging to shear deformations. In Ref. [9], it is suggested that $\chi = T_{\mathrm{eff}}/T_Z$ relaxes according to

$$\dot{\chi} = \alpha_1 e^{-1/\chi}\Gamma\chi\left(1 - \frac{\chi}{\chi_{\infty}}\right) + \alpha_2 e^{-\beta/\chi}\rho\chi\left(1 - \frac{\chi}{\chi_T}\right), \quad (25)$$

where α_1, α_2, and β are constants. The first term describes the change of T_{eff} connected to the configurational degrees of freedom associated with the STZs. It tends to drive the effective temperature toward a steady-state value χ_{∞} in the presence of plastic flow with a rate proportional to the total number density $\propto \Lambda_{\infty} = \exp(-1/\chi)$ of STZs times Γ. The second term describes the change of T_{eff} connected to the configurational degrees of freedom if all other defects are taken into account that characterize the nonequilibrium state. Consequently, the effective temperature relaxes toward the bath temperature, i.e., $\chi_T = T/T_Z$. The number density of all defects (including the STZs) is $\propto \exp(-\beta/\chi)$, where $\beta k_B T_Z$ is a typical defect formation energy, and the relaxation rate per defect (or per volume) is assumed to be proportional to ρ.

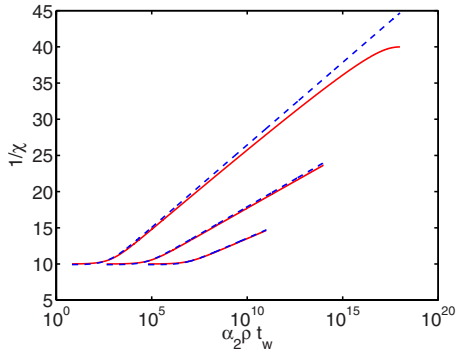

FIG. 6. (Color online) Numerical solution of Eq. (25) for $\Gamma = 0$ and the parameters $\alpha_2 = 1$, $\rho = 1$, and $\chi_T = 0.025$ and three values of $\beta = 1$, 1.5, and 2 (top to bottom). Also shown is the asymptotic result Eq. (27) in the aging regime (dashed lines).

For studying aging behavior, Eqs. (23) and (25) together with Eq. (24) have to be solved in the stress-step protocol, and in addition Eq. (19) in the constant-strain-rate protocol. In the absence of loading ($\Gamma = 0$) during the waiting time t_{w}, aging as reflected in a change of T_{eff} can only occur for nonzero values of ρ. Accordingly, we need to assume $\rho > 0$ below T_g here. If ρ is considered to be independent of T_{eff} (and time), integration of Eq. (25) yields

$$E_1\{\beta[\chi_T^{-1} - \chi(t_{\mathrm{w}})^{-1}]\} = E_1(\beta[\chi_T^{-1} - \chi_0^{-1}]) + \alpha_2 \exp(-\beta/\chi_T)\rho t_{\mathrm{w}}, \quad (26)$$

where $E_1(x) = \int_x^{\infty} du \exp(-u)/u$ is the exponential integral and χ_0 the initial value after the quench. As long as T_{eff} is not close to T (i.e., $\beta[\chi_T^{-1} - \chi(t_{\mathrm{w}})^{-1}] = \beta\chi_T^{-1}[1 - T/T_{\mathrm{eff}}(t_{\mathrm{w}})] \gg 1$), we can use the asymptotic relation $E_1(x) \sim \exp(-x)/x$ for large $x = \beta[\chi_T^{-1} - \chi(t_{\mathrm{w}})^{-1}]$ in Eq. (26). If we further replace x by $\beta\chi_T^{-1}$ in the denominator of $\exp(-x)/x$, we obtain

$$\frac{1}{\chi(t_{\mathrm{w}})} \sim \frac{1}{\beta}\ln(e^{\beta/\chi_0} + \alpha_2\beta\chi_T^{-1}\rho t_{\mathrm{w}}) \quad (27)$$

for $\alpha_2\rho t_{\mathrm{w}} \ll (\chi_T/\beta)[\exp(\beta/\chi_T) - \exp(\beta/\chi_0)]$. Figure 6 shows the validity of this approximation [31]. It implies a power-law decrease of the STZ density, $\Lambda_{\infty}(t_{\mathrm{w}}) = \exp[-1/\chi(t_{\mathrm{w}})] \sim (\alpha_2\beta\chi_T^{-1}\rho t_{\mathrm{w}})^{-1/\beta}$ in the aging regime $(\chi_T/\beta)\exp(\beta/\chi_0) \ll \alpha_2\rho t_{\mathrm{w}} \ll (\chi_T/\beta)[\exp(\beta/\chi_T) - \exp(\beta/\chi_0)]$. This is an interesting feature, since values $\beta > 1$ naturally generate sublinear aging behavior in the state variable χ. On the other hand, the onset of the aging regime at waiting times $\propto \rho^{-1}\exp(\beta/\chi_0)$ can be orders of magnitude larger than microscopic times, in disagreement with what is commonly observed in simulations and experiments.

To explore temperature effects, we proceed as in Sec. III and vary the relaxation time scale $\tau = a(T)t_0$ together with

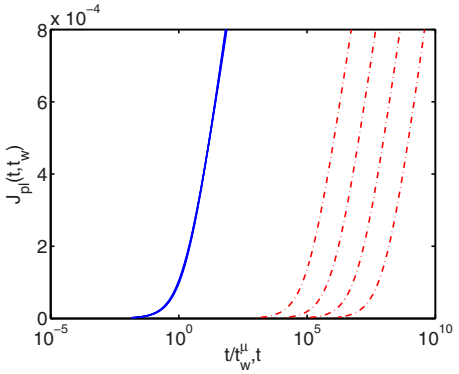

FIG. 7. (Color online) Compliance curves (red, dot-dashed) for several wait times $t_w=10^5-10^8$ and $\sigma_{\text{ext}}=0.05$ in the effective time formulation of the STZ theory. The other parameters are $\tau=1/\rho=1$, $\chi_T=0.01$, and $\beta=1$. The compliance curves collapse (blue, solid) when time is rescaled with t_w^{μ}; here we achieve the best collapse with $\mu=0.97$.

$\chi_T=T/T_Z$. In order to explore the effect of subaging in the STZ density, we furthermore consider the possibility of a temperature-dependent parameter $\beta(T)>1$ at lower temperatures, but the physical interpretation of such a variation is not yet obvious. The relaxation rate ρ should also vary with T. However, when rescaling time by τ (or $1/\rho$), only the product $\rho\tau$ enters the equations of motion, so that a change of ρ can be attributed to a simple rescaling of all time scales. We therefore keep ρ constant here.

We solve Eqs. (23), (25), and (19) numerically with the initial condition $\epsilon_{\text{pl}}(0,t_{\text{w}})=0$ [and $\sigma(0,t_{\text{w}})=0$ in the constant-strain-rate protocol]. The value for $\chi(0,t_{\text{w}})$ follows from Eq. (26). For the constants we choose $\alpha_1=\alpha_2=1$, and $\chi_\infty=0.5$ independent of shear rate. The physically relevant regime should appear if we let $\chi(0,0)=0.1\leqslant\chi_\infty$ for the initial condition and set $\chi_T\ll 1$ [9] (Ref. [16] suggests to set $\chi_\infty=\chi_T$ when $\chi_T>\chi_\infty$ in the low shear rate limit; however, all situations studied here obey $\chi_T<\chi_\infty$).

A. Creep compliance

As before, we begin by solving for the plastic strain rate at fixed applied stress σ_{ext} and obtain creep compliance curves for different waiting times shown in Fig. 7. Aging is now described not by reduced STZ transition rates, but instead by a reduced effective temperature $\chi(0,t_w)$. We observe that this approach can also generate a scaling behavior with waiting time, but the scaling form for the compliance is different: for small σ we have basically $\dot{\epsilon}_{pl}=\text{const}/t$ from Eq. (23), yielding $\epsilon_{\text{pl}}(t)\sim\ln(t)$. This form also does not agree well with the Kohlrausch form Eq. (3).

B. Peak stress

The constant-strain-rate protocol provides a richer and more stringent test on the predictions of the theory. Stress-strain curves shown in Fig. 8 for different waiting times are

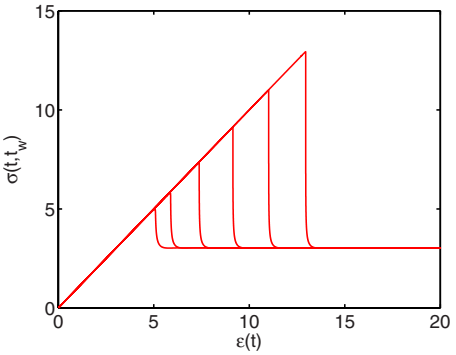

FIG. 8. (Color online) Stress-strain curves for several waiting times $t_{\text{w}}=10^2-10^8$ (bottom to top) at fixed strain rate $\dot{\epsilon}_{\text{ext}}=0.1$. All other parameters are as in Fig. 7.

qualitatively similar to those of Fig. 2. Again we find a peak stress that increases with waiting time t_w and a plateau stress independent of t_w. Similarly, curves in Fig. 9 for varying rate and constant t_w show that both σ_{max} and σ_{ss} increase with increasing strain rate. As in Fig. 3, we also find two regimes of weak and strong rate sensitivity for small and large strain rates, respectively. There is, however, a notable difference between the two models: the difference between the peak and plateau stress (overshoot) does not increase with increasing rate as in Fig. 3, but appears to remain constant in the limit of large rates. This is due to the fact that peak stress and plateau stress exhibit the same logarithmic rate dependence. A likely cause of this behavior here is that we have taken χ_∞ to be a constant independent of shear rate. For quantitative modeling of amorphous solids, a nontrivial rate dependence of χ_∞ should be assumed [9,16]. Coupling χ_∞ to $\dot{\epsilon}_{\text{ext}}$ in a way similar to Eq. (9), so that χ_∞ increases with rate, will induce a different rate dependence of the two stresses.

In analogy to Fig. 4, we summarize trends of the peak and plateau stress with waiting time and strain rate for several different temperatures in Fig. 10. Lower temperatures are achieved by increasing τ and increasing β. As can be seen, the effective time formulation generates very comparable results. Figure 10(a) shows that the peak stress rises logarithmically with waiting time for all temperatures, and the offset can again be adjusted by choosing τ. Interestingly, we observe that subaging of the STZ density causes a decrease of

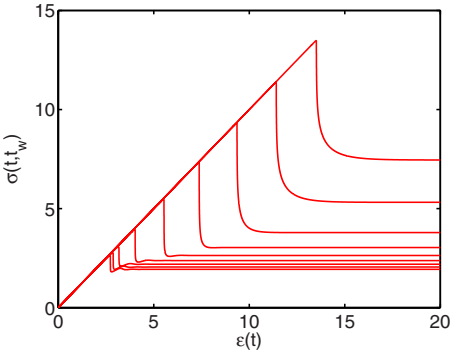

FIG. 9. (Color online) Stress-strain curves for varying strain rates $10^{-7}-10^{1}$ (bottom to top) and fixed $t_{\text{w}}=10^3$. All other parameters are as in Fig. 7.

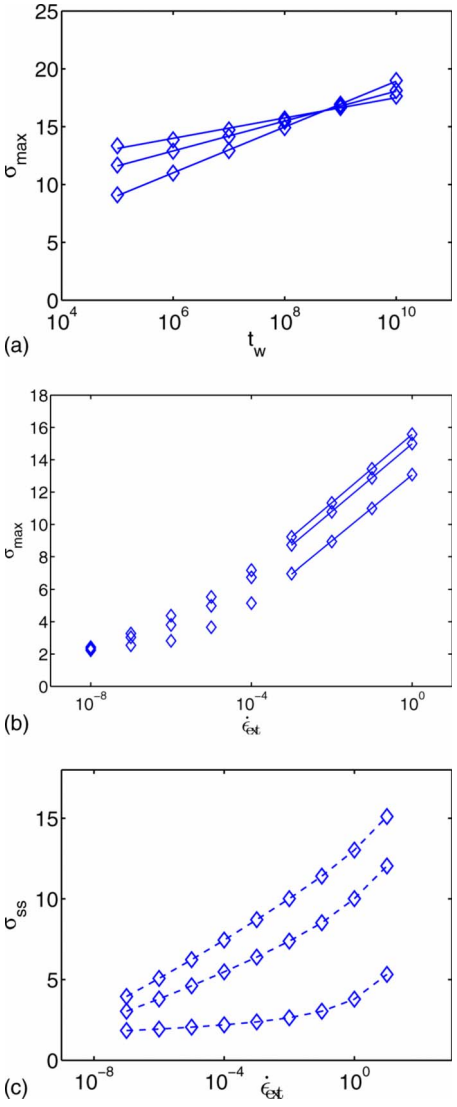

FIG. 10. (Color online) (a) Peak stress against wait time at $\dot{\epsilon}_{\rm ext}=0.1$ for three different "temperatures" represented by the parameter sets ($\beta=1$, $\tau=1$, $\chi_T=0.01$), ($\beta=1.5$, $\tau=1000$, $\chi_T=0.005$), ($\beta=2$, $\tau=20\,000$, $\chi_T=0.001$) (from bottom to top). Solid lines show logarithmic fits to the data and have slopes $\sigma^{(1)}_{\rm max}\propto 1/\beta$. (b) Peak stress against rate for the same three temperatures at $t_{\rm w}=10^6$. The solid lines have slope $\sigma^{(2)}_{\rm max}=0.91$. (c) Steady-state plateau stress against strain rate for the same three temperatures.

the logarithmic slope $\sigma^{(1)}_{\rm max}\propto 1/\beta(T)$, just as subaging of the relaxation time was found to reduce $\sigma^{(1)}_{\rm max}$ [see Fig. 4(a)]. Inspecting the peak stress $\sigma_{\rm max}$ as a function of rate in Fig. 10(b), we find a regime of logarithmic rate dependence with slope $\sigma^{(2)}_{\rm max}$ if $t_w>1/\dot{\epsilon}_{\rm ext}$ and a crossover into a weaker dependence for $t_w<1/\dot{\epsilon}_{\rm ext}$. The rate sensitivity in this regime depends again on the value of β. The plateau stress $\sigma_{\rm ss}$ exhibits the same two regimes of rate dependence.

Finally, we confirm the scaling behavior of the peak stress with waiting time and rate in Fig. 11. Plotting the peak stress against the product $\dot{\epsilon}t_w$ collapses all data onto a common curve.

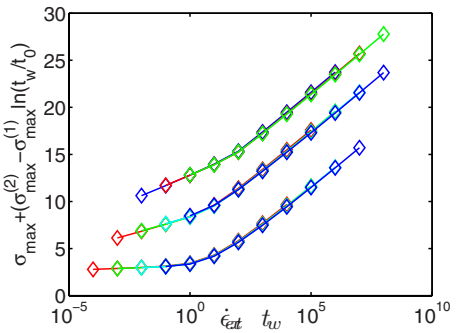

FIG. 11. (Color online) Scaling plot of the peak stress as predicted by Eq. (4) for the three different "temperatures" analyzed in Figs. 10(a) and 10(b) and several waiting times.

V. DISCUSSION

The two models with a slowing down of STZ transition rates (model A) and a relaxation of the effective temperature-controlled STZ density (model B) are both capable of capturing most of the qualitative aging features observed in computer simulations and experiments. The similarity of the results obtained in both models can be understood from the time evolution of the plastic strain in the STZ theory. According to Eq. (5), it does not matter whether aging reduces the STZ density or the transition rates between STZ states, since the plastic strain rate is proportional to the number of STZ transitions per unit time and volume. Whether fewer STZs rearrange at a fixed rate, or whether the same number of STZs rearrange at slower rates, the net effect for the strain is the same.

In the present work, temperature effects enter into the STZ transition rates only via a temperature-dependent prefactor [see Eq. (7)]. An alternative would be to employ Eyring-like expressions of the form $R_{\pm}(\sigma)=\exp[-T_E/T(1\mp\sigma/\sigma_0)]$ as suggested in Ref. [9]. In this case, the logarithmic slope $\sigma^{(1)}_{\rm max}$ in Figs. 4 and 10 would no longer depend on μ or β alone, but would also depend linearly on T. However, it has been pointed out that the Eyring expression predicts several other trends for the yield stress that are inconsistent with observations [32,33], among them a vanishing rate dependence at low temperatures and a temperature-independent yield stress in the small strain rate limit. For this reason and for ease of comparison, we have chosen to use Eq. (7) for both models.

In the stress-step protocol, both models A and B successfully account for the typical scaling behavior seen in the compliance, but they do not reproduce the typical stretched exponential form of the scaling function. This should not be surprising in view of the mean-field rate equations used so far, where the time evolution of the many different STZs is represented by an averaged behavior. Disorder fluctuations in transition and defect forming energies are expected to yield broad distributions of the characteristic times entering the models and these are expected to modify the form of the scaling function.

In the constant-strain-rate protocol, the two models reproduce an increase of the peak stress with waiting time and a relaxation toward a $t_{\rm w}$-independent plateau stress for contin-

ued straining into the stationary state. In both models, the associated loss of memory is caused by the energy dissipation under loading, which drives the primary transition rate between STZ states or the effective temperature toward t_w-independent values. An increase of the overshoot stress with the strain rate is not seen in model B when a rate-independent value of χ_∞ is used. However, this feature would be missing in model A also if we had not assumed a strain-rate-dependent limiting value τ_∞ of the primary relaxation time in Eq. (9).

It is worth noting that the dissipation mechanism is also active during the initial loading period. It thus should also affect the time needed to reach the peak stress in the constant-strain-rate protocol or the characteristic time for plastic strain to build up in the constant stress-step protocol. However, for typical parameter values used in the present study, the influence of dissipation during the initial loading seems to be too weak for generating a visible rejuvenation effect. It is nevertheless an attractive idea to associate rejuvenation (or reduced aging) with a facilitated stress (or strain) response by dissipated energy. Further studies are necessary to clarify this possibility in more detail.

More generally, the question arises as to which of the two models more closely describes the microscopic dynamics on a coarse-grained level. A problem in the effective temperature formulation is the onset of the aging regime, which can be much larger than microscopic times. Another conceptual difficulty is that the effective temperature is not directly accessible, while the characteristic time scale τ can be determined in simulations (and in experiments if τ is assumed to correspond to the scale of the main structural α-relaxations). The effective temperature was shown to describe a nonequilibrium steady-state system [13], but there is no comparable evidence yet that it also describes the transient behavior in model B in the same way. On the other hand, the effective temperature formulation captures many details of the behavior of bulk metallic glasses very successfully and consistently [9]. It is impressive in its simplicity, since only two rate equations for $\epsilon_{pl}(t)$ and $\chi(t)$ are needed to describe the dynamics. Moreover, in view of many experimental studies on memory effects in plastic deformation of solids, where defect concentrations have been shown to play a crucial role, it is likely that a change of the STZ density is a key factor in understanding aging memory.

It seems that the different physical mechanisms underlying models A and B are both important to obtain a satisfactory description of the aging dynamics. In future work, we will perform a quantitative comparison between the predictions of the two models and the simulation data described in Sec. II in order to provide tighter constraints on their applicability. More important is, however, to clarify what really happens on the molecular scale. Simulations are needed to answer this question.

ACKNOWLEDGMENTS

We would like to thank J. S. Langer, M. L. Manning, and M. Warren for many helpful discussions. J.R. gratefully acknowledges financial support from the National Science and Engineering Research Council of Canada (NSERC).

[1] D. Turnbull and M. Cohen, J. Chem. Phys. **52**, 3038 (1970).
[2] F. Spaepen, Acta Metall. **25**, 407 (1977).
[3] A. S. Argon, Acta Metall. **27**, 47 (1979).
[4] M. L. Falk and J. S. Langer, Phys. Rev. E **57**, 7192 (1998).
[5] M. L. Falk, Phys. Rev. B **60**, 7062 (1999).
[6] J. S. Langer and L. Pechenik, Phys. Rev. E **68**, 061507 (2003).
[7] J. S. Langer, Phys. Rev. E **70**, 041502 (2004).
[8] L. Pechenik, Phys. Rev. E **72**, 021507 (2005).
[9] J. S. Langer, Phys. Rev. E **77**, 021502 (2008).
[10] J. Bauschinger, Zivilingenieur **27**, 289 (1881).
[11] The ratio of the annihilation rate per STZ and the creation rate per volume determines a limiting value of the population densities that they would reach in the absence of preferable alignment under loading.
[12] L. F. Cugliandolo, J. Kurchan, and L. Peliti, Phys. Rev. E **55**, 3898 (1997).
[13] L. Berthier and J.-L. Barrat, Phys. Rev. Lett. **89**, 095702 (2002).
[14] P. Ilg and J.-L. Barrat, Europhys. Lett. **79**, 26001 (2007).
[15] T. K. Haxton and A. J. Liu, Phys. Rev. Lett. **99**, 195701 (2007).
[16] J. S. Langer and M. L. Manning, Phys. Rev. E **76**, 056107 (2007).
[17] Y. Shi, M. B. Katz, H. Li, and M. L. Falk, Phys. Rev. Lett. **98**, 185505 (2007).
[18] J. Rottler and M. O. Robbins, Phys. Rev. Lett. **95**, 225504 (2005).
[19] W. Kob and H. C. Andersen, Phys. Rev. E **51**, 4626 (1995).
[20] M. Warren and J. Rottler, Phys. Rev. E **76**, 031802 (2007).
[21] L. C. E. Struik, *Physical Aging in Amorphous Polymers and Other Materials* (Elsevier/North-Holland, Amsterdam, 1978).
[22] In other contexts, the term "rejuvenation" is used when there is a (possibly apparent) complete loss of aging after external perturbations and not a reduction of the slowing down as reflected in a decrease of μ. The concept of distinguishing between perturbation-induced rejuvenation and overaging effects by comparing relaxation times with those in unperturbed reference states goes back to the pioneering work by Struik [21].
[23] J. Rottler and M. Warren, Eur. Phys. J. Spec. Top. **161**, 55 (2008).
[24] K. Chen and K. S. Schweizer, Phys. Rev. Lett. **98**, 167802 (2007).
[25] W. Kob and J.-L. Barrat, Phys. Rev. Lett. **78**, 4581 (1997).
[26] A. Lemaitre, Phys. Rev. Lett. **89**, 195503 (2002).
[27] Using free volume theory, one may write $R_\pm(\sigma) = R\exp(-V_\mp/v_f)$, where v_f is the mean free volume and $V_\pm = V_0\exp(\pm\sigma/\sigma_V)$ are "activation volumes" for the STZ transitions [4]. For $\sigma/\sigma_V \ll 1$, this gives $R_\pm(\sigma) = \exp(\mp\sigma/\sigma_0)/\tau$ with $\tau = \exp(V_0/v_f)/R$ and $\sigma_0 = (v_f/V_0)\sigma_V$.
[28] C. Derec, A. Ajdari, and F. Lequeux, Eur. Phys. J. E **4**, 355

(2001).
[29] F. Varnik, L. Bocquet, and J.-L. Barrat, J. Chem. Phys. **120**, 2788 (2004).
[30] J. Lu, G. Ravichandran, and W. L. Johnson, Acta Mater. **51**, 3429 (2003).
[31] For $t_w > (\chi_T/\beta)[\exp(\beta/\chi_T) - \exp(\beta/\chi_0)]$, $\chi^{-1} \sim \{\chi_T^{-1} - \beta^{-1}\exp[-\alpha_2 \exp(-\beta/\chi_T)]\rho t_w\}$ or $\Lambda_\infty \sim \exp(-1/\chi_T)\{1 + \beta^{-1}\exp[-\alpha_2 \exp(-\beta/\chi_T)]\rho t_w\}$, i.e., the STZ density Λ_∞ relaxes exponentially toward its equilibrium value $\exp(-1/\chi_T)$ with a rate $\propto \rho \exp(-\beta/\chi_T)$.
[32] K. Chen and K. S. Schweizer, Europhys. Lett. **79**, 26006 (2007).
[33] J. Rottler and M. O. Robbins, Phys. Rev. E **68**, 011507 (2003).